Study of the adsorption activity of Fe_3O_4 synthesized by the solvothermal method in relation to doxorubicin

Andrii Kusyak[1], Nataliya Kusyak[1], Liudmyla Storozhuk[2], Alla Petranovska[2], Petro Gorbyk[2], Nataliya Korniichuk[2], Iryna Yanovych[1]

[1]*Department of chemistry, Ivan Franko Zhytomyr State University, 40 Velyka Berdychivska St, 10008 Zhytomyr, Ukraine*

[2]*Chuiko Institute of Surface Chemistry, National Academy of Sciences of Ukraine, 03164 Kiev, Ukraine*

Abstract

The solvothermal method synthesized magnetite (Fe_3O_4) and investigated the processes of immobilization of the cytostatic drug doxorubicin (DOX) on its surface in the medium of 0.9% NaCl solution. The size and morphology (transmission electron microscopy (TEM), crystalline phase magnetite formation (X-ray diffraction analysis (XRD), FTIR spectroscopy) and magnetic properties (vibration magnetometer (VSM), specific surface area and pore size were determined by the method of nitrogen thermal desorption were investigated for the synthesized samples. The adsorption processes were studied and the high adsorption activity of the Fe_3O_4 nanoparticles (MNPs) surface with respect to DOX was established in the model physiological environment. According to the studies, the adsorption equilibrium time is 45–90 min with up to 80% DOX extraction and maximum adsorption capacity (A_{max}) 17.5 mg·g^{-1}. The analysis of kinetic dependences and DOX adsorption isotherms using mathematical models that take into account the chemical interaction in the system indicates the monomolecular nature of adsorption (Freundlich model). Obtained MNPs can be potentially suitable for oncology applications specifically in the targeted drug delivery and adsorption materials of intracorporeal and extracorporeal detoxification of the body.

Keywords

Doxorubicin,·magnetite,·nanoparticles,·solovthermal method, adsorption

Introduction

The development of nanotechnology opens up new opportunities to create targeted forms of drug delivery, the ability to accumulate and visualize the accumulation of a drug in the pathological area, and to effectively transport the active substance. For these purposes, Fe_3O_4 nanoparticles are particularly attractive because the drugs on their basis are characterized by increased efficacy, minimal side effects, improved bioavailability and controlled drug release. That is why the development and implementation of new methods for the synthesis of nanosized materials based on Fe_3O_4 with predicted parameters and properties remain an actual. (Wu et al. 2015; Sun et al. 2017).

The using of drugs immobilized on the surface of Fe_3O_4 nanoparticles (MNPs) in the chemotherapeutic practice involves the preliminary modification of the surface of MNPs. (Akbarzadeh et al. 2012; Liang et al. 2016; Yang et al. 2016; Abramov et al. 2016, 2017; Turanska et al. 2016; Unsoy et

al. 2014; Sadighiana et al. 2014; Kanamala et al.2016; Shen et al. 2018; Chen et al. 2014). Due to the modification of MNPs new centers are formed to provide specific interaction with the target cell receptors [Price et al. 2018; Yew et al. 2018] and the absence of aggregate on is fixed (Chae et al. 2015).

In addition to nanoparticles which containing drugs on the surface or in bulk, nanoparticles with hollow structures and different morphologies are used (Zhu et al. 2007; Zeng et al. 2010; Xie et al. 2018; Albinali et al. 2019; Lou et al. 2008; Fan et al. 2007; Guan et al. 2010; Jia et al. 2013; Cheng et al. 2010; Jia et al. 2008; Hu et al. 2008; Quanguo et al. 2014; Cheng et al. 2009; Liangli et al. 2018).

Among the chemical methods for producing monodisperse hollow/mesoporous Fe_3O_4 nanoparticles, the solvothermal method is of particular importance because it allows to obtain particles with satisfactory magnetic characteristics, morphology and sizes that can be used for biomedical applications. Since the solvothermal synthesized MNPs have high surface energy and high surface tension and are capable of agglomeration, optimization of synthesis conditions, selection of reagents and their ratios remain relevant. Synthesis of Fe_3O_4 is carried out from compounds of iron (Fe^{3+} salts) in the glycols medium, in particular ethylene glycol (EG), which, according to (Smith 2002; Kozakova et al. 2015) is dehydrated to form acetaldehyde, which is a reducting agent for Fe^{3+} ions. The process takes place in the presence of stabilizers, precipitants and structure-forming agents at high temperatures (Wu et al. 2015; Madrid et al. 2014; He et al. 2018; Ooi et al. 2015; Zhang et al. 2011; Dosovitskii et al. 2017; Gao et al. 2010).

Doxorubicin, an anticancer anthracycline antibiotic, was selected as the model chemotherapeutic agent because of its wide spectrum of antitumor activity. A major drawback associated with DOX chemotherapy involves its significant severe side effects, which could be dramatically reduced by the use of cytocompatible drug nanocarriers, and therefore the use of MNPs with loaded DOX opens new perspectives in the clinical practice. The main aim of this work was to study the processes of adsorption immobilization of the anticancer drug DOX on MNPs synthesized by a solvothermal method with a size of 100 nm.

Experimental

Materials

Ferric chloride ($FeCl_3 \cdot 6H_2O$), ethylene glycol ($HOCH_2CH_2OH$), sodium acetate (CH_3COONa), Ethanol (C_2H_5OH) (Merck), DOX (Teva, Pharmaceutical Industries Ltd.). All materials were used without any treatment during nanomaterials synthesis.

Preparation and characterisations of MNPs

Magnetite nanosphears were prepared by solvothermal method (He et al. 2018). Iron chloride and sodium acetate in equil volume (1:4) with ethylene glycol addition were put to avtoclave for solvothermal treatment at 200 °C for 10 h. After cooling to room temperature black precipitate was collected by magnet and washed with deionised water and ethanol. The product was dried at 80 °C for 24 h.

The cristal structure of nanoparticles was determinated by XRD (perfomed using DRON-4-07 diffractometer with Cu/Kα radiation (λ = 0.1542 nm) and Ni filter). Surface studies of nanodispersed samples were performed by FTIR spectroscopy (Perkin Elmer Fourier Spectrometer, model 1720X).

Investigation of morphology and size distribution of MNPs were performed in water solutions. The size and shape of the MNPs were determined by transmission electron microscopy (JEOL 1200-EX, Japan) with a tungsten filament operating at a 120 kV acceleration voltage. The TEM samples were diluted in deionizer water, dropping it onto a carbon coated copper grid (EM Resolutions Ltd) and were dried at room temperature for 12 h. Specific surface area and pore size were determined by the method of nitrogen thermal desorption (KELVIN 1042 Sorptometer).

Optical density measurements, absorption spectra and concentration of DOX in solutions were performed by spectrophotometric analysis (Spectrometer Lambda 35 UV/Vis Perkin Elmer Instruments). The magnetization of the samples was measured using a vibrating magnetometer at a frequency of 228 Hz at room temperature as described in (Abramov et al. 2017). Samples for research were dry demagnetized polydisperse materials. For comparing Ni sample and Fe_3O_4 (98%) nanoparticles ("Nanostructured & Amorphous Materials Inc", USA) were used. The measurement error did not exceed 2.5%.

The study of DOX adsorption onto the MNPs surface

To investigate the processes of DOX immobilization on the surface of MNPs, a series of samples with different concentrations of DOX in the range of 0.01 – 0.2 mg ml^{-1} were produced.

Adsorption of DOX was performed for 2 h in in batch and dynamic mode at room temperature. The amount of adsorbed drug on the surface of the nanocomposites was determined by measuring the concentration of DOX solutions before and after adsorption. The concentration was determined by spectrophotometry measurements at λ = 480 nm using calibration graph. The adsorption capacity was calculated using Eq.(1):

$$A = (C_0 - C_{eq}) \cdot V/g \quad (1)$$

where A (mg g^{-1}) is the amount adsorbed. C_0 and Ceq (mg ml^{-1}) are the initial and equilibrium concentration of the DOX solution. V (ml) is the volume of the solution, g (g) is the mass of absorbent used.

The removal efficiency of DOX (R) was obtained with Eq. (2):

$$R, \% = [(C_0 - C_{eq})/ C_0] \cdot 100 \quad (2)$$

Results and discussion

Characterization of MNPs

The synthesized MNPs were investigated by complex of phisical methods. The study of MNPs surface by the method of nitrogen thermal desorption showed the presence of a significant specific surface area and pores.

BET surface area – 59.57 m^2 g^{-1}

Langmuir surface area – 77.18 m^2 g^{-1}

Total pore volume – 358.84 mm^3 g^{-1}

Micropore volume – 0.00 mm^3 g^{-1}

The XRD patterns of obtained MNPs are shown in Fig. 1. The diffraction peaks are characteristic of the spinel-like structure without any peaks of another phases. The diffraction pattern of the synthesized

sample is characterized by the three most intense reflexes at 2θ = 35.5°; 41.5°; 50.1°. The data found (Fig. 1) are in good agreement with the crystallographic data of the magnetite phases (JCPDS № 88-315). Calculating with Debye–Scherrer formula from peak (311), the average sizes of the crystallite were determined to be 21.6 nm.

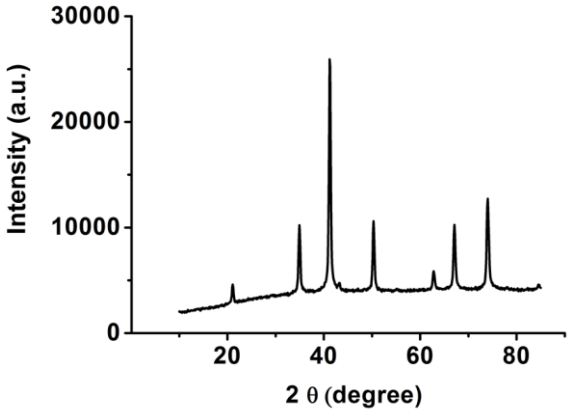

Fig. 1 XRD patterns of MNPs

Dried MNPs were characterized by FTIR. Figure 2 shows the spectra of the as-prepared Fe_3O_4. The characteristic band in the range 640 cm^{-1} is attributed to the stretching vibration bands associated to the iron-oxygen bonds (Fe–O). The absorbance bands at 895, 976, 1050 cm^{-1} and 1121 cm^{-1} attributed to the deformation vibrations of Fe–OH groups. A band at 1655 cm^{-1} attributed to the O–H stretching vibration modes. A broad band between 2800 cm^{-1} and 3500 cm^{-1} related to the OH stretching vibration modes of water and indicates the presence of hydrogen bonds.

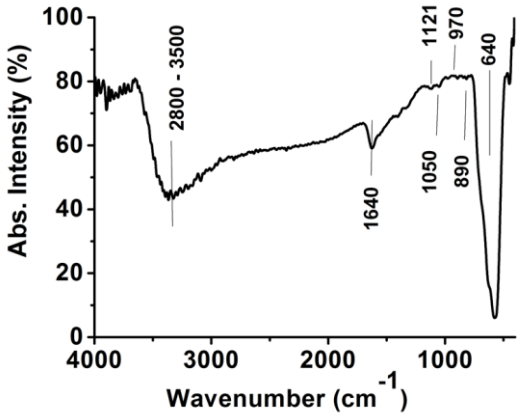

Fig. 2 FTIR spectra of MNPs

Synthesized Fe_3O_4 nanoparticles were observed in the TEM. TEM images (Fig. 3) show Fe_3O_4 nanoparticles obtained from solvatermal method are monodisperse and have spheric shape with an average diameter of 90 ± 10 nm without significant aggregation.

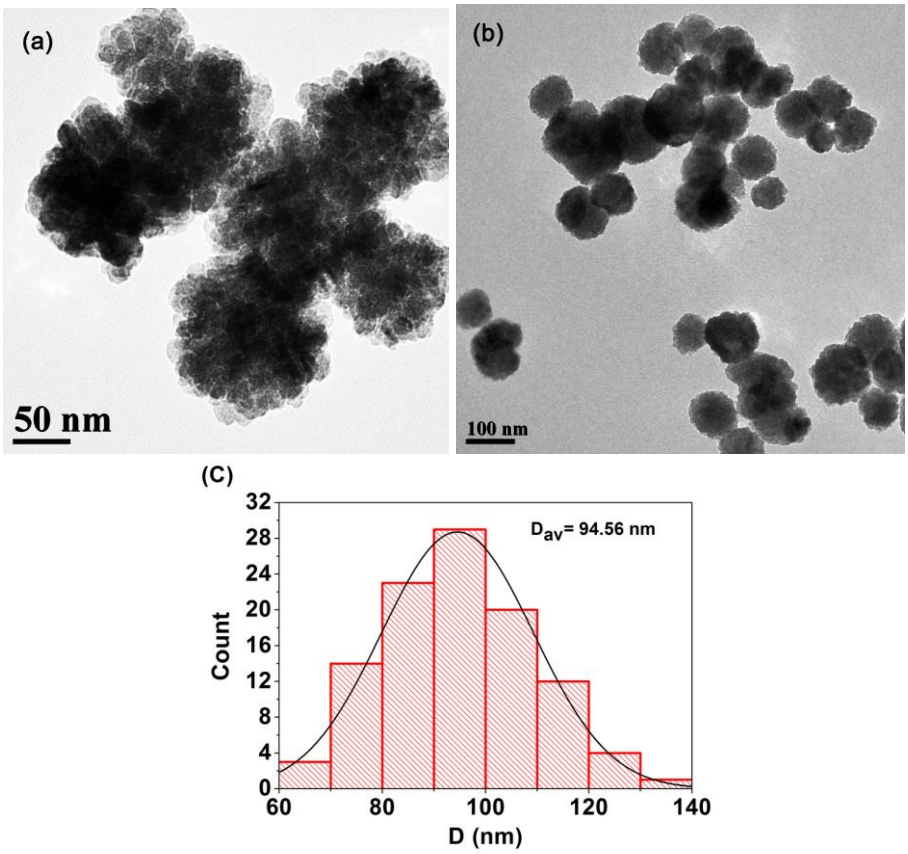

Fig. 3 TEM images of MNPs. Scale bar: **a** 50 nm; **b** 100 nm; **c** the corresponding particle size distribution

The magnetization of MNPs as a function of the magnetic field is represented in Fig. 4.

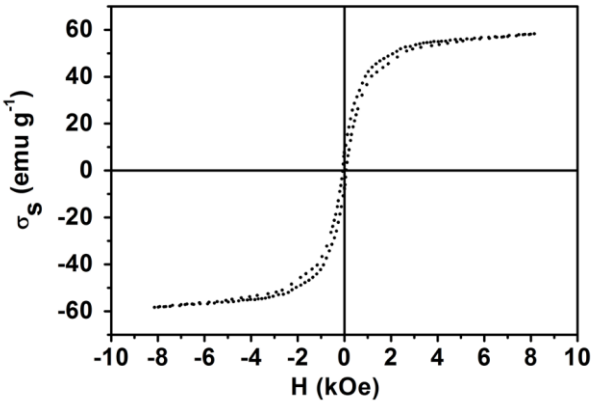

Fig. 4 Hysteresis loops for synthesized MNPs

Magnetic measurements on Fe_3O_4 nanoparticles indicate that the particles are superparamagnetic at room temperature with a coercivity (H_c) of 81 Oe. The measured saturation magnetization (σ_s,) is 60.1 emu g^{-1}. Determination of the magnetic properties of the synthesized MNPs showed that the samples had narrow hysteresis loops. It indicate low energy losses during magnetization. (Fig. 4, Table 1)

Table 1 Magnetic characteristics of MNPs

Sample	H_c, kOe	σ_s, emu g^{-1}	$\sigma_{H=8\ kOe}$,emu g^{-1}	σ_r, emu g^{-1}	σ_r/σ_s	α_{Fe3O4}^{calc}, %
Fe_3O_4	0.081	60.1	58.4	7.28	0.121	100

Adsorption of DOX onto MNPs surface

Adsorption kinetics

In this work, two common kinetic models were used to investigate the adsorption kinetics of DOX onto sorbent. Experiments were carried out for different contact times (15 – 180 min) with initial concentration of DOX 0.01 – 0.075 mg ml^{-1} and pH = 7.

In order to establish the main sorption capacity, the dependence of sorption C (DOX) on contact time and concentration was investigated. The kinetic curves of DOX sorption were constructed (Fig. 5a, b).

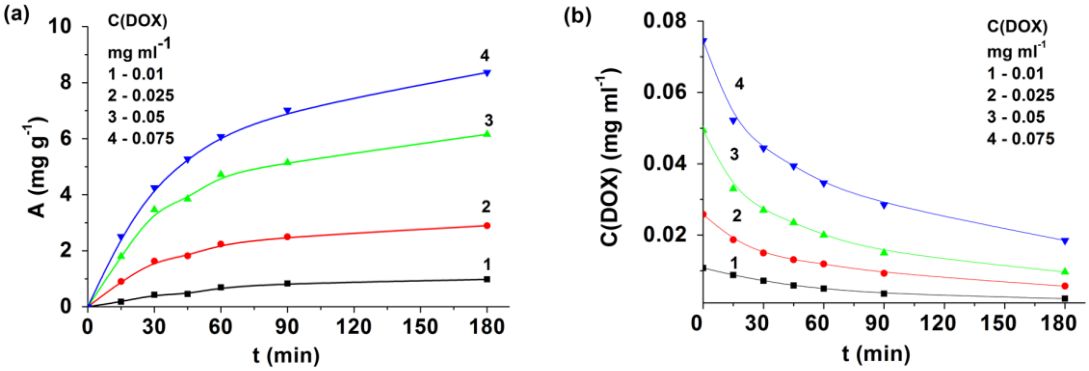

Fig. 5 Experimental kinetic curves of DOX sorption on the surface of MNPs

The experimental results indicate a sufficiently high surface affinity for DOX. The removal efficiency was of up to 80%. The maximum amount of DOX was adsorbed in the first 45 min. The experimental kinetic curves of DOX adsorption on MNPs have been analyzed using kinetic equations and models. The parameters of pseudo-first-order and pseudo-second-order kinetic models were obtained from the fitted straight lines (Fig. 6a, b) and are shown in the table (Table 2).

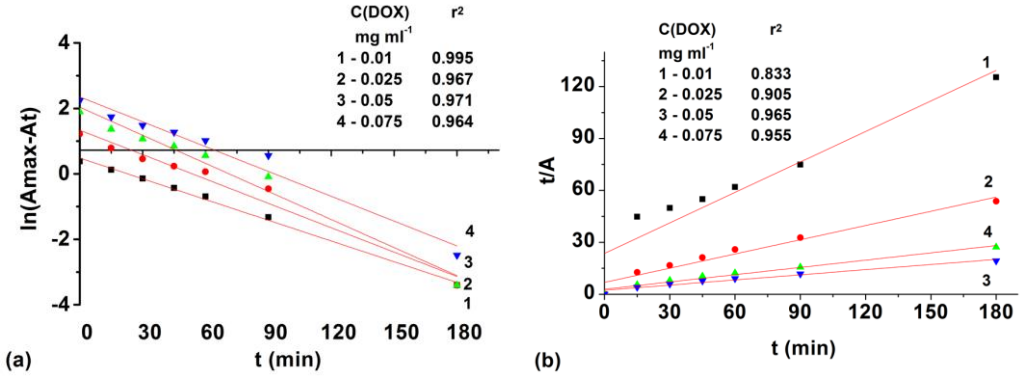

Fig. 6 a Pseudo-first and **b** pseudo-second order kinetics of DOX adsorption on the MNPs

Table 2 Equilibrium rate constant, the amount adsorbed at equilibrium, and correlation coefficients adsorption kinetic of DOX on MNPs

			Pseudo-first order kinetic			Pseudo-second order kinetic		
MNPs, mg ml^{-1}	DOX, mg ml^{-1}	$A_{eq,exp}$, mg g^{-1}	k_1, min^{-1}	$A_{eq,cal}$, mg g^{-1}	r^2	k_2, g mg^{-1} min^{-1}	$A_{eq\ cal}$, mg g^{-1}	r^2
6	0.010	1.44	0.0211	1.49	0.995	0.0124	1.13	0.833
6	0.025	3.35	0.0248	3.41	0.967	0.0098	2.9	0.905
6	0.050	6.62	0.0286	6.67	0.971	0.0062	5.87	0.965
6	0.075	9.42	0.0253	9.49	0.964	0.0038	8.17	0.955

The values of the theoretically calculated sorption capacity are as close as possible to the experimentally obtained. So sorption capacity values and higher correlation coefficients ($r^2 \geq 0.95$) give preference to a pseudo-first-order model that corresponds to the adsorption of the DOX cationic form at pH 7 (Roik et al. 2017) (Table 2).

Adsorption isotherms

The experimental data were investigated with Langmuir and Freundlich adsorption isotherms. For obtaining of DOX adsorption isotherm on the Fe_3O_4 surface 5 ml solutions of DOX with concentrations of 0.01 − 0.2 mg ml^{-1} were added to the test samples at 20 °C for 180 min in static mode. The experimental results are given in Fig.7.

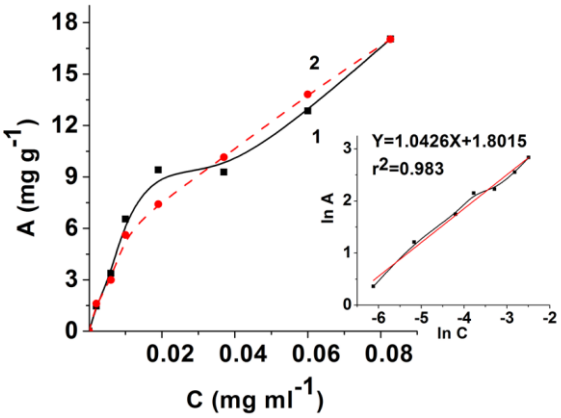

Fig. 7 Isoterms of DOX adsorption on MNPs obtained from adsorption experiment **(1)** and calculated with Freundlich **(2)** model. The inset shows the linear plot form of the equation Freundlich

It was seen that increasing the equilibrium concentration of DOX does not lead to adsorption saturation of the Fe_3O_4 surface within the current concentrations. This can be explained by the porosity of the surface and the structure of the DOX.

According to the experimental data at different intervals of equilibrium concentrations the amount of sorption (*A*) and the the removal efficiency (*R*) were determined. A_{max} = 17.5 mg g^{-1}, *R* was up to 80%.

Experimental values of the adsorption capacity were used to construct an adsorption isotherm close to the L-type isotherms (Fig. 7). To determine the adsorption process and the interaction of DOX with the

MNPs surface, the possibility of using classical Langmuir and Freundlich models was evaluated (Table 3). Conformity checks were performed by the linearization method.

Table 3 Parameters of DOX adsorption on MNPs calculated using Langmuir and Freunlich models

Equilibrium adsorption model	Langmuir	Freunlich
Calculated adsorption parameters	K_L – 39.65	K_F – 86.1
	A_{max} – 19.39	*1/n* – 1.53
	r^2 – 0.835	r^2 – 0.982

For DOX activity in sorption processes is determined by the amino-group (*5*) (Fig.8), the state of protonation which depends on the pH of the medium. In saline medium (pH − 6.8), the DOX fraction with protonated amino groups is maximum (Roik et al. 2017), at the same time, under these conditions, only non-ionized hydroxyl groups are available on the Fe_3O_4 surface (Warren 2013), which does not promote ion-ion interactions and correspondingly high sorption properties.

At the same time, according to the structure of the DOX molecule, where there are various chemically active functional groups (Fig. 8), which are responsible for the formation of hydrogen bonds between OH-groups *(3)* and electron-donor oxygen atoms (*1* and *2*), and also keto-groups (*4*), with basic properties, may form intramolecular and intermolecular hydrogen bonds. Therefore, there is probably an interaction between the non-ionized hydroxyl groups of the surface and the active centers in the DOX structure, which accounts for the correspondence of the sorption isotherm of the Freundlich model.

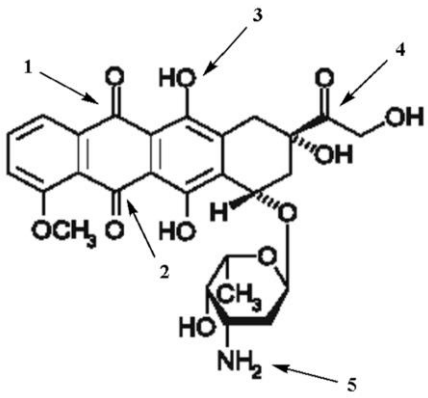

Fig. 8 Structural formula of DOX molecule: electron-donor oxygen atoms **(1, 2)**; OH-groups **(3)**; keto-groups **(4)**; amino-group **(5)**

Conclusions

Porous MNPs were synthesized by the solvothermal method and were investigated by a complex of physical methods. It is established that the magnetic characteristics correspond to crystalline magnetite.

MNPs show sufficiently high sorption activity to DOX (A_{max} = 17.5 mg g^{-1}, *R* up to 80%) in saline medium. According to kinetic studies, the sorption equilibrium time of DOX sorption is 45 − 90 min.

Analysis of the kinetic dependences and isotherms of DOX adsorption indicates the monomolecular nature of adsorption (Freundlich model).

The results of experimental studies testify that the synthesized porous MNPs are promising for use in medicine as adsorption materials for intracorporeal (enterosorption) and extracorporeal detoxification and targeted drug delivery.

Competing interests

The authors declare that they have no competing interests.

All authors read and approved the final manuscript.

References

Abramov MV, Kusyak AP, Kaminskiy OM, Turanska SP, Petranovska AL, Kusyak NV, Gorbyk PP (2017) Magnetosensitive nanocomposites based on cisplatin and DOX for application in oncology. In: Reimer A. (ed.) Horizons in World Physics, Nova Science Publisher, New York, pp 1−56

Abramov NV, Turanska SP, Kusyak AP, Petranovska AL, Gorbyk PP (2016) Synthesis and properties of magnetite/hydroxyapatite/DOX nanocomposites and magnetic liquids based on them. J Nanostruct Chem 6:223−233. https://doi.org/10.1007/s40097-016-0196-z

Akbarzadeh A, Mikaeil H, Zarghami N, Mohammad R, Barkhordari A, Davaran S (2012) Preparation and in vitro evaluation of DOX-loaded Fe_3O_4 magnetic nanoparticles modified with biocompatible copolymers. Int J Nanomed 7:511−526. https://doi.org/10.2147/ijn.s24326

Albinali KE, Zagho MM, Deng Y, Elzatahry AA (2019). A perspective on magnetic core–shell carriers for responsive and targeted drug delivery systems. Int J Nanomed 14:1707−1723. https://doi.org/10.2147/IJN.S193981

Chae HS, Piao SH, Choi HJ (2015) Fabrication of spherical Fe_3O_4 particles with a solvothermal method and their magnetorheological characteristics. J Ind Eng Chem 29:129−133. https://doi.org/10.1016/j.jiec.2015.02.027

Chen F, Liu R, Xiao S, Lin M (2014) One-step solvothermal synthesis of epichlorohydrin-modified magnetic Fe_3O_4 microspheres in ethylene glycol. Mater Lett 130: 101−103. https://doi.org/10.1016/j.matlet.2014.05.022

Cheng K, Peng S, Xu C, Sun S (2009) Porous hollow Fe_3O_4 nanoparticles for targeted delivery and controlled release of cisplatin. J Am Chem Soc 131:10637−10644. https://doi.org/10.1021/ja903300f

Cheng W, Tang K, Qi Y, Sheng J, Liu Z (2010) One-step synthesis of superparamagnetic monodisperse porous Fe_3O_4 hollow and core-shell spheres. J Mater Chem 20:1799−1805. https://doi.org/10.1039/b919164j

Dosovitskii AE, Grishechkina EV, Mikhlin AL, Kirdyankin DI, Novotortsev VM (2017) Effect of the synthesis conditions on the size of MNPs produced by high-temperature reductive hydrolysis. Russ J Inorg Chem 62: 702−710. https://doi.org/10.1134/S0036023617060055

Fan HJ, Gösele U, Zacharias M (2007) Formation of nanotubes and hollow nanoparticles based on Kirkendall and diffusion processes: a review. Small 3:1660−1671. https://doi.org/10.1002/smll.200700382

Gao G, Shi R, Qin W, Shi Y, Xu G, Qiu G, Liu X (2010) Solvothermal synthesis and characterization of size-controlled monodisperse Fe_3O_4 nanoparticles. J Mater Sci 45: 3483−3489. https://doi.org/10.1007/s10853-010-4378-7

Guan J, Mou F, Sun Z, Shi W (2010) Preparation of hollow spheres with controllable interior structures by heterogeneous contraction. Chem Commun 46:6605−6607. https://doi.org/10.1039/c0cc01044h

He Q, Liu J, Liang J, Liu X, Ding Z, Tuo D, Li W (2018) Sodium acetate orientated hollow/mesoporous MNPs: facile synthesis, characterization and formation mechanism. Appl Sci 8: 292. https://doi.org/10.3390/app8020292

Hu P, Yu L, Zuo A, Guo C, Yuan F (2008) Fabrication of monodisperse magnetite hollow spheres. J Phys Chem C 113:900−906. https://doi.org/10.1021/jp806406c

Jia B, Gao L (2008) Morphological transformation of Fe_3O_4 spherical aggregates from solid to hollow and their self-assembly under an external magnetic field. J Phys Chem C 112:666−671. https://doi.org/10.1021/jp0763477

Jia Y, Yu XY, Luo T, Zhang MY, Liu JH, Huang XJ (2013) Two-step self-assembly of iron oxide into three-dimensional hollow magnetic porous microspheres and their toxic ion adsorption mechanism. Dalton Trans 42:1921−1928. https://doi.org/10.1039/c2dt32522e

Kanamala M, Wilson WR, Yang M, Palmer BD, Wu Z (2016) Mechanisms and biomaterials in pH-responsive tumour targeted drug delivery. Biomaterials 85:152−167. https://doi.org/10.1016/j.biomaterials.2016.01.061

Kozakova Z, Kuritka I, Kazantseva NE, Babayan V, Pastorek M et al. (2015) The formation mechanism of iron oxide nanoparticles within the microwave-assisted solvothermal synthesis and its correlation with the structural and magnetic properties. Dalton Trans 44:21099−21108. https://doi.org/10.1039/C5DT03518J

Liang PC, Chen YC, Chiang CF, Mo LR, Wei SY, Hsieh WY, Lin WL, (2016) DOX-modified magnetic nanoparticles as a drug delivery system for magnetic resonance imaging-monitoring magnet-enhancing tumor chemotherapy. Int J Nanomed 11:2021−2037. https://doi.org/10.2147/IJN.S94139

Liangli C, Yuren J, Zhencheng C (2018) Hollow Fe_3O_4/graphene oxide nanocomposites as novel rapamycin carrier: formulation optimization and *in vitro* characterization. J Nanosci Nanotechno 18:3067−3076. https://doi.org/10.1166/jnn.2018.14674

Lou XW, Archer LA, Yang Z (2008) Hollow Micro-/Nanostructures: Synthesis and Applications. Adv Mater 20:3987−4019. https://doi.org/10.1002/adma.200800854

Madrid SI, Pal U, Jesús FS (2014) Controlling size and magnetic properties of Fe_3O_4 clusters in solvothermal process. Advances in Nano Research 2:187−198. https://doi.org/10.12989/anr.2014.2.4.187

Ooi F, DuChene JS, Qiu J, Graham JO, Engelhard MH, Cao G, Gai Z, Wei WD (2015) A facile solvothermal synthesis of octahedral Fe_3O_4 nanoparticles. Small 11: 2649−2653. https://doi.org/10.1002/smll.201401954

Price PM, Mahmoud WE, Al-Ghamdi AA, Bronstein LM (2018) Magnetic Drug Delivery: Where the Field Is Going. Front Chem 6:619. https://doi.org/10.3389/fchem.2018.00619

Quanguo H, Jun L, Chunyan H, Zhaohui W (2014) A nanoscale system for remarkably enhanced drug delivery based on hollow magnetic particles encapsulated within temperature-responsive poly(methylmethacrylate). Sci Adv Mater 6:387−398. https://doi.org/10.1166/sam.2014.1728

Roik NV, Belyakova LF, Dziazko MO (2017) Adsorption of antitumor antibiotic DOX on MCM-41-type silica surface. Adsorpt Sci Technol 35: 86−101. https://doi.org/10.1177/0263617416669504

Sadighiana S, Rostamizadeh K, Hosseini-Monfareda H, Hamidi M (2014) DOX-conjugated core–shell MNPs as dual-targeting carriers for anticancer drug delivery. Colloid Surface B 117:406−413 https://doi.org/10.1016/j.colsurfb.2014.03.001

Shen C, Wang X, Zheng Z, Gao C, Chen X, Zhao S, Dai Z (2018) DOX and indocyanine green loaded superparamagnetic iron oxide nanoparticles with PEGylated phospholipid coating for magnetic resonance with fluorescence imaging and chemotherapy of glioma. Int J Nanomed 14:101−117. https://doi.org/10.2147/IJN.S173954

Smith WB (2002) Ethylene glycol to acetaldehyde-dehydration or a concerted mechanism. Tetrahedron 58:2091−2094. https://doi.org/10.1016/S0040-4020(02)00103-5

Sun X, Sun S (2017) Preparation of Magnetic Nanoparticles for Biomedical Applications. In: Petrosko S, Day E (eds) Biomedical Nanotechnology. Methods in Molecular Biology, Humana Press, New York, pp. 73−90. https://doi.org/10.2147/IJN.S24326

Turanska SP, Kusyak AP, Petranovska AL, Gorobez SV, Turov VV, Gorbyk PP (2016) Cytotoxic activity of magnet-quided DOX-based nanocomposites with Saccharomyces cerevisiae cells as an example. Himia Fizika ta Tehnologia Poverhni 7:236−245. https://doi.org/10.15407/hftp07.02.236

Unsoy G, Khodadust R, Yalcin S, Mutlu P, Gunduz U (2014) Synthesis of DOX loaded magnetic chitosan nanoparticles for pH responsive targeted drug delivery. Eur J Pharm Sci 62:243–250. https://doi.org/10.1016/j.ejps.2014.05.021

Warren C (2013*)* Synthesis, characterization, and functionalization of magnetic iron nanoparticles for enhanced biological applications. Dissertation, Virginia Commonwealth University.

Wu W, Wu Z, Yu T, Jiang C, Kim WS (2015) Recent progress on magnetic iron oxide nanoparticles: synthesis, surface functional strategies and biomedical applications. Sci Technol Adv Mater 16:023501. https://doi.org/10.1088/1468-6996/16/2/023501

Xie W, Guo Z, Gao F, Gao Q, Wang D, Liaw B, Cai Q, Sun X, Wang X, Zhao L (2018). Shape-, size- and structure-controlled synthesis and biocompatibility of iron oxide nanoparticles for magnetic theranostics. Theranostics 8:3284−3307. https://doi.org/10.7150/thno.25220

Yang Y, Guo Q, Peng J, Su J, Lu X, Zhao Y, Qian Z (2016) DOX-conjugated heparin-coated superparamagnetic iron oxide nanoparticles for combined anticancer drug delivery and magnetic resonance imaging. J Biomed Nanotechnol 12:1963−1974. https://doi.org/10.1166/jbn.2016.2298

Yew YP, Shameli K, Miyake M et al (2018) Green biosynthesis of superparamagnetic magnetite Fe_3O_4 nanoparticles and biomedical applications in targeted anticancer drug delivery system: A review. Arab J Chem. https://doi.org/10.1016/j.arabjc.2018.04.013

Zeng Y, Hao R, Xing B, Hou Y, Xu Z (2010) One-pot synthesis of Fe_3O_4 nanoprisms with controlled electrochemical properties. Chem Commun 46:3920−3922. https://doi.org/10.1039/c0cc00246a

Zhang W, Shen F, Hong R (2011) Solvothermal synthesis of magnetic Fe_3O_4 microparticles via self-assembly of Fe_3O_4 nanoparticles. Particuology 9: 179−186. https://doi.org/10.1016/j.partic.2010.07.025

Zhu LP, Xiao HM, Fu SY (2007) Template-free synthesis of monodispersed and single-crystalline cantaloupe-like Fe_2O_3 superstructures. Cryst Growth Des 7:177−182. https://doi.org/10.1021/cg060454t